JOURNAL OF SYNCHROTRON RADIATION

Volume 28 (2021)

Supporting information for article:

Side-bounce beamlines using single-reflection diamond monochromators at Cornell High Energy Synchrotron Source

Stanislav Stoupin, Thomas Krawczyk, David Sagan, Alexander Temnykh, Louisa Smieska, Arthur Woll, Jacob Ruff, Aaron Lyndaker, Alan Pauling, Brendan P. Croom and Edward B. Trigg

Supporting information

I. INFLUENCE OF CRYSTAL LATTICE DISTORTIONS ON THE REFLECTED BEAM PROFILES

A. 220 reflector at 2B beamline

A set of 20 CVD diamond crystal plates was studied using X-ray rocking curve topography in the double crystal configuration to quantify distortions of the crystal lattice (the studied plate set as the second crystal reflecting X-rays in the Laue geometry). These distortions manifested themselves primarily as substantial variation of the rocking curve peak position across the plates. Maps of the effective radius of curvature in the scattering plane were calculated using spline interpolation of the peak position. The main crystal selection criterion was the presence of a crystal region with a size comparable to that of the footprint of the incident X-ray beam where the radius of curvature attained maximum possible value (i.e., minimimal lattice bending)[1].

Figure 1 shows results of rocking curve topography for a CVD diamond plate chosen as the 220 reflector in the monochromator of the 2B beamline. The figure also shows two profiles of the reflected beams at 13 m downstream the monochromator, where the incident undulator-produced X-ray beam illuminated two distinct regions on the plate. The topographs represent maps of the peak intensity (I_R^{peak}) normalized by the maximum observed value, the RMS width of the rocking curve ($\Delta\theta_\sigma$), the peak position of the rocking curve ($\delta\theta_m$) and the effective radius of curvature (R). The scattering plane is oriented along the x-axis on the topographs. The rocking curve topography was performed using a custom-built setup based on Cu rotating anode X-ray source. The setup was operating at a fraction of the source's maximum possible power. This explains the noisy appearance of the topographs (most noticeably, I_R^{peak} and $\Delta\theta_\sigma$). Nevertheless, variation of the peak position ($\delta\theta_m$) is determined reliably. It appears to be more uniform in the upper portion of the crystal (marked by black dashed rectangle). The effective radius of curvature attains values of $R > 30$ m in the center of the region. During commissioning of the monochromator while the undulator beam was illuminating this region the reflected beam had a profile with a single lobe of intensity as shown by the corresponding panel in the Figure (marked by an arrow pointing towards the dashed rectangle). On the contrary, the adjacent region on the bottom (white solid rectangle) appears to be less uniform on the peak position $\delta\theta_m$ topograph. The R topograph in this region has a pattern showing two separated narrow regions with large values. The corresponding profile of the reflected/monochromatized beam (marked by an arrow pointing towards the white solid rectangle) had two distinct lobes of intensity. This example illustrates the influence of the lattice bending profile on the shape of the reflected beam and further justifies the crystal selection procedure.

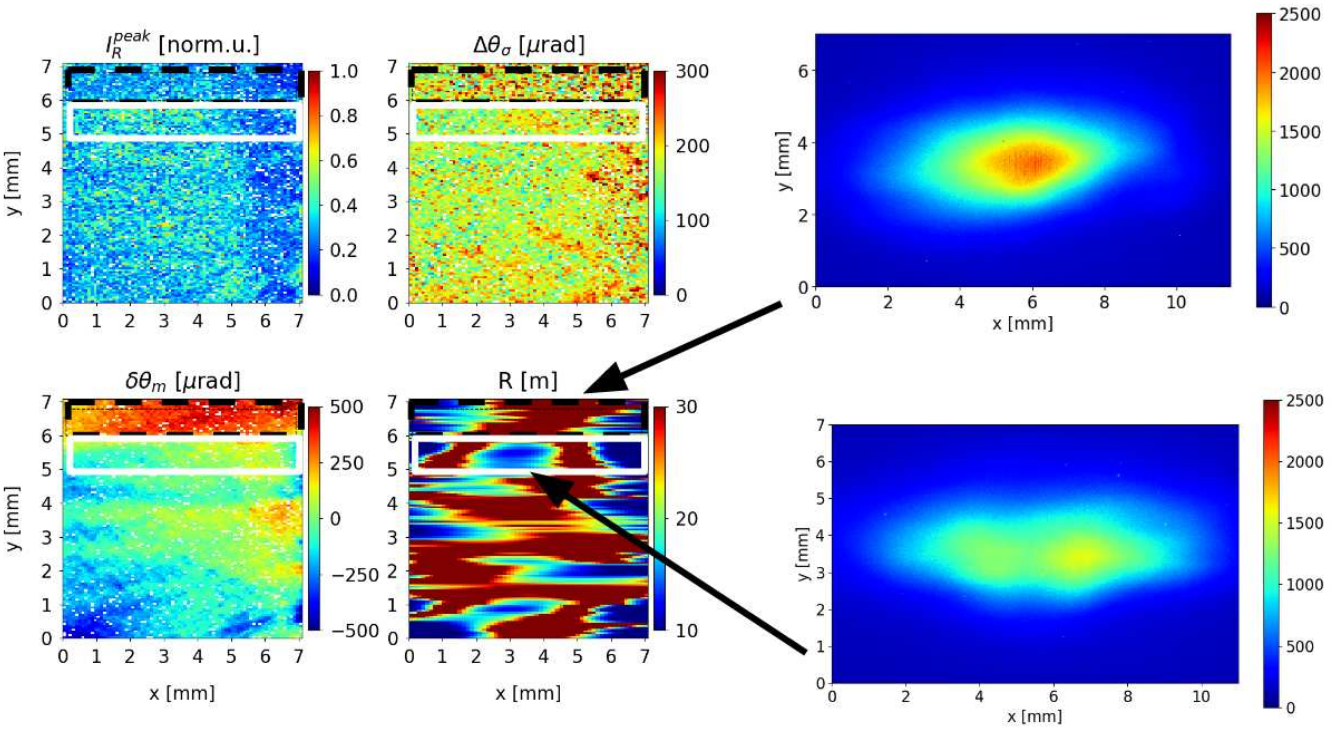

FIG. 1: Rocking curve topographs for a CVD diamond plate chosen as the 220 reflector in the monochromator of the 2B beamline: peak intensity (I_R^{peak}) normalized by the maximum observed value, the RMS width of the rocking curve ($\Delta\theta_\sigma$), the peak position of the rocking curve ($\delta\theta_m$) and the effective radius of curvature (R). The scattering plane is oriented along the x-axis. A more uniform region of the plate illuminated with the undulator beam during commissioning of the monochromator (black dashed rectangle) produces a single lobe of intensity in the reflected beam profile at 13m downstream the monochromator, while the less uniform region (white solid rectangle) produces two lobes of intensity in the reflected beam profile under the same conditions.

B. CVD reflectors at 3B beamline

Figure 2 shows the profiles of the monochromatized X-ray beams of the 3B beamline monochromator (a-c) (also shown in Fig. 6(a-c) of the paper) along with the peak position ($\delta\theta_m$) and the RMS curve width $\Delta\theta_\sigma$ rocking curve topographs of the corresponding CVD reflectors (d-f). The crystal regions illuminated by the incident undulator beam are marked by the dashed lines (the regions contained inside the $\approx$ 1-mm-wide stripe in between the two lines shown for each topograph). The appearance of the beam profiles can be qualitatively explained by the character of lattice distortions revealed in the $\delta\theta_m$ topographs. For the 220 and 400 reflectors the overall orientation of the lattice along the incident beam remains approximately uniform (along x-axis). The profiles of the corresponding reflected beams (Fig.2(a,c)) are not tilted substantially unlike the one of the 131 reflector (Fig.2(b)). This substantial tilt of the beam profile can be qualitatively explained as follows. The azimuthal angle of the 131 reflector is offset by 18°, which sets the 131 reciprocal vector in the horizontal scattering plane (the crystal plate has 001 edge orientation). The footprint of the incident beam (inclined at 18°) crosses a crystal region, which represents approximate equal orientation of the lattice (the inclined contour of equal orientation visible by elevated (red) values of $\delta\theta_m$ in Fig. 2(e)). Thus, the incident beam footprint experiences steep lattice curvature along its longer dimension. This results in defocusing and elongation of the beam profile in the direction of the steepest curvature. Thus, the resulting beam profile acquires the tilted appearance. In addition, the sense of this tilt is inverted by the X-ray mirror (the profiles of the beams upon reflection from the beamline's X-ray mirror are shown in Fig 2(a-c)). We note that the azimuthal offset of the crystal in the opposite sense 18° (i.e., setting the crystal for the $\bar{1}31$ reflection) would likely reduce the tilt of the beam profile. In principle, the tilt of the profile can be controlled by choice of the reflector. However, manufacturing of a CVD diamond reflector with a desired profile of the crystal lattice can be a non-trivial problem.

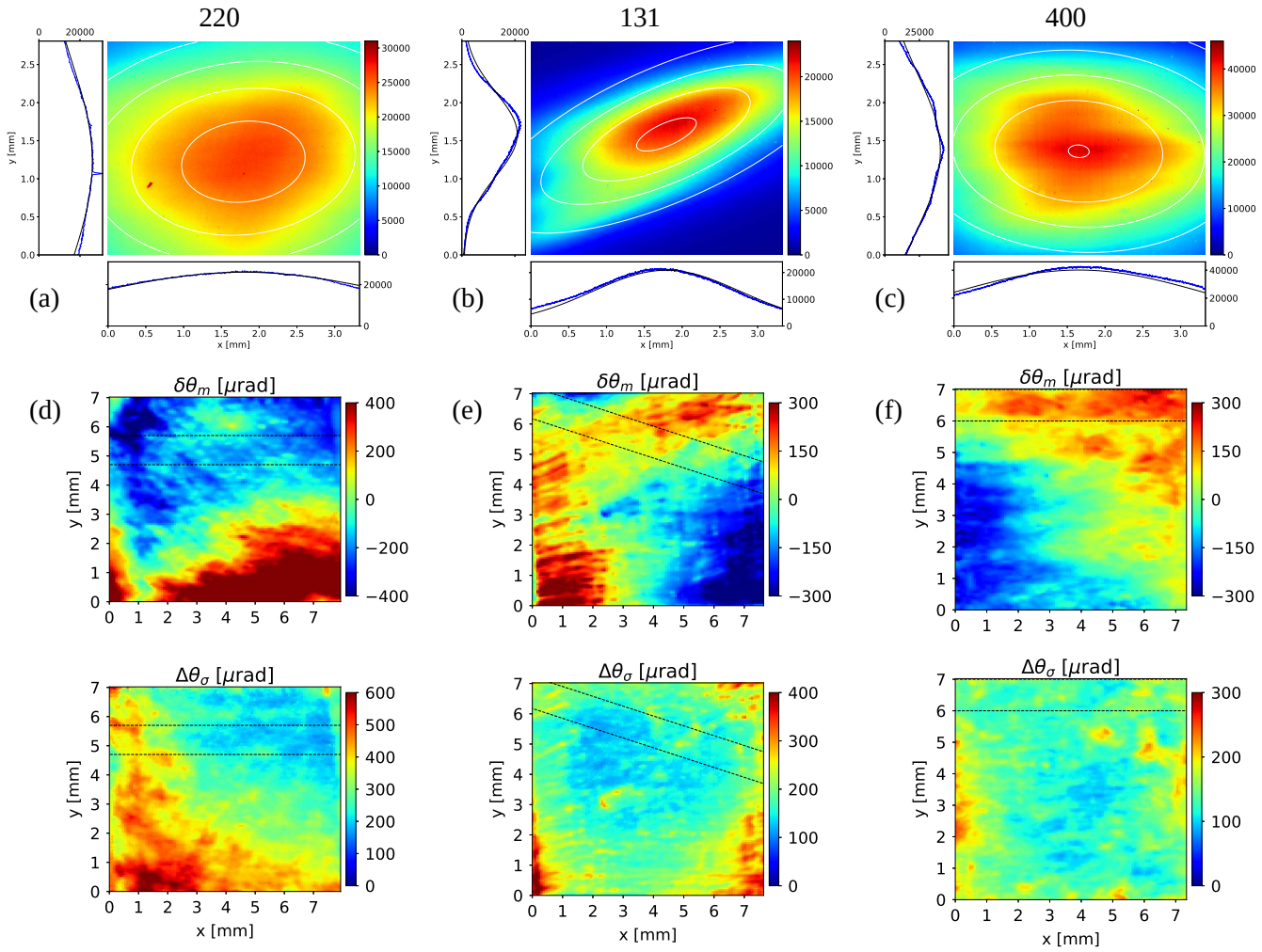

FIG. 2: Profiles of the monochromatized X-ray beams of the 3B beamline monochromator (a-c) (as shown in Fig. 6(a-c) of the manuscript) correlated with the peak position ($\delta\theta_m$) and the RMS curve width $\Delta\theta_\sigma$ rocking curve topographs of the corresponding CVD reflectors (d-f). The scattering plane is oriented along the x-axis. The region in between the dashed lines in (d-f) represents the footprint of the incident undulator beam during commissioning of the monochromator. The tilted appearance of the 131 reflector beam profile (b) is due to crossing the contour of equal lattice orientation by the incident beam footprint (see text for details).

II. ON THE EFFECTIVE ENERGY BANDWIDTH OF THE CVD REFLECTORS

A certain average value of the rocking curve width $< \Delta\theta_\sigma >$ can be ascribed to the crystal areas illuminated by the incident beam using the $\Delta\theta_\sigma$ topographs shown in Fig. 2(d-f). The average value for the intrinsic energy bandwidth of the CVD crystals can be estimated as

$$\frac{\Delta E}{E} = \frac{< \Delta\theta_\sigma >}{\tan\theta_B} \tag{1}$$

The resulting values of $\Delta E/E$ range from about 1×10^{-3} to 2×10^{-3} (FWHM) depending on the crystal. The values of ΔE remain on the same order of magnitude but exceed the energy bandwidths measured using the 2×2 mm aperture at the distance of 8 m from the monochromator for the 3B beamline (Table 6 of the paper). This can be attributed to the fact that the average intrinsic curve width $\simeq 2.35\times < \Delta\theta_\sigma > \simeq$ 350-600 μrad (FWHM) is greater than the angular acceptance of the aperture $\frac{2mm}{8m} = 250$ μrad. Only a fraction of the total radiation bandwidth delivered by the CVD crystal is transmitted through the aperture. This observation suggests that further increase in

the intrinsic angular width (mosaicity) of the diamond crystals will not yield an increase in the flux delivered through the aperture.

---

[1] S. Stoupin, T. Krawczyk, Z. Liu, and C. Franck, Crystals **9**, 396 (2019).